P4.5 IMPACT OF SOIL MOISTURE INITIALIZATION ON A SIMULATED FLASH FLOOD

C. Travis Ashby* and William R. Cotton
Colorado State University, Fort Collins, CO

1. INTRODUCTION

During the evening hours of 28 July 1997 an extreme precipitation event caused flash flooding in Fort Collins, Colorado. The storm produced more than 10" of localized precipitation between 2330Z July 28 and 0005Z July 29 (Doesken and McKee, 1998). The synoptic conditions surrounding this event were very similar to those of the Big Thompson flood of 1976 and the Rapid City flood of 1972 (Maddox et. al., 1978). Each of these events involved very moist low-level flow impinging on an orographic barrier along the western periphery of a surface high, weak to moderate moist mid-level flow and a 500 hPa negatively tilted ridge axis in the vicinity of the affected area. The Regional Atmospheric Modeling System (RAMS) (Pielke et. al., 1992) is being used to improve our understanding of the physical mechanisms involved in heavily precipitating, quasi-stationary convection. The objective is not necessarily to reproduce the Fort Collins storm precisely, but rather to better understand the simulated mechanisms for extreme precipitation generation given differing initial conditions. The initial atmospheric condition for this day is known, post facto, to correspond to a potential flash-flood-producing environment and therefore serves as a logical starting point for investigating model-generated extreme precipitation.

2. MODEL CONFIGURATION

The atmospheric model used in this research is RAMS Version 3b (Pielke et al., 1992). The model grid utilizes an oblique-stereographic projection in the horizontal and a terrain following vertical coordinate. Four, two-way interactive nested grids are used with grid spacing of 80, 20, 5, and 1.667 km on Grids 1, 2, 3 and 4 respectively. Parameterizations for moist-convection, radiative transfer, turbulent diffusion, surface-layer processes, and soil and vegetation interactions are also included and utilized. The convective parameterization used is a modified-Kuo scheme and is employed only on Grid 1. The remaining grids (2, 3 and 4) rely on explicitly simulated precipitation processes. The soil model employs 11 variably spaced vertical levels reaching a maximum depth of 50 cm.

Two simulations are performed with the initial conditions differing only in the initial soil moisture distribution. Simulation A utilizes the 0-10 cm and 10-200 cm volumetric soil moisture from the 12Z July 28 1997 operational ETA model analysis. Simulation B uses the Antecedent Precipitation Index (API) method of estimating antecedent soil moisture conditions (Saxton and Lenz, 1967). This method utilizes a three-month record of gauge precipitation measurements to estimate point values of the mean, upper 30-cm soil moisture content. These values are then objectively analyzed onto the model grids using a Barnes scheme with a 0.9 response at 200-km wavelength. Significant initial soil moisture differences are found with the API method yielding 18% average soil saturation on the third nested grid compared to 54% in the ETA analysis. The initial atmospheric fields (temperature, pressure, vapor mixing ratio and horizontal winds) are identical between simulations. Each simulation is initiated at 12Z July 28, 1997 with Grids 1-3 active, and are executed to 15Z with cloud water as the only form of condensate allowed. This is done to prevent initial model adjustment dynamics from artificially modifying the initial soil moisture distribution. At 15Z full microphysics is activated and integrated to 18Z at which point Grid 4 is inserted. The simulations are then allowed to proceed to 05Z July 29, 1997 and are terminated at this time.

3. BOUNDARY LAYER EVOLUTION

Table 1 shows the simulated, area-averaged surface variables and integral convective parameters at 1900Z and 2000Z. The averaging area extends from 105.1°W to 104.6°W and from 39.6°N to 40.8°N. This area includes Fort Collins, Denver and Greeley, and is intended to characterize the simulated boundary layer evolution immediately to the east of the Front Range foothills. The effect of the more moist soil conditions in Sim. A includes a 6.4°C cooler surface temperature and a 4.9°C warmer surface dewpoint temperature at 2000Z. The Sim. A temperature, dewpoint, and dewpoint-depression agree more closely with the Fort Collins afternoon surface observations than does that of Sim. B. One consequence of the large dewpoint depression in Sim. B is the close proximity of the LCL and LFC relative to the mid-level, westerly, downslope-component wind. This results in virtually no cloud cover (not shown) east of the Front Range foothills while Sim. A produces broken cloud conditions over the same area in better agreement with surface and satellite observations. The lack of cloud cover in Sim. B results in a higher surface available energy relative to Sim. A (Table 1). Hence, the differences in soil moisture initialization lead not only to a difference in the partitioning of available energy but also to variations in the available energy itself, due to suppression or enhancement of the low-level cloud field. The higher available energy (AE) in Sim. B, coupled with the lower evaporation fraction (EF) results in a much higher sensible heat flux and consequently a deeper boundary layer (Table 1) relative to Sim. A. In fact, despite the higher available energy in Sim. B, the surface θ_e remains nearly constant during the afternoon hours (Table 1) as a result of dry air entrainment into the daytime boundary layer. By 2000Z, Sim. B exhibits lower CAPE relative to Sim. A, a result of the low-level drying associated with entrainment, in addition to a warmer, drier and deeper boundary layer.

Corresponding Author Address:
C. Travis Ashby, Colorado State University, Department of Atmospheric Science, Fort Collins, CO, 80523-1371.
E-mail: ashby@atmos.colostate.edu

Variables	1900Z		2000Z	
	Sim. A	Sim. B	Sim. A	Sim. B
$\overline{T}$ (°C)	18.9	24.7	19.5	25.9
$\overline{T}_d$ (°C)	17.6	14.1	18.3	13.4
$\overline{u}$ (m/s)	-3.68	-6.87	-4.00	-6.43
$\overline{v}$ (m/s)	+0.20	-0.26	+0.48	+1.01
LCL (m-AGL)	615	1340	590	1569
$\overline{\theta}_e$ (K)	349.0	347.5	351.8	347.5
Available Energy (W/m^2)	375	598	376	565
Evap. Fraction	0.90	0.28	0.93	0.34
Bound. Layer Depth (m)	~370	~900	~370	~1300
LFC (m-AGL)	1657	2309	831	2012
$CAPE$ (J/kg)	594	632	1057	722
CIN (J/kg)	9	24	2	10
Precipitable Water (cm)	3.51	3.30	3.68	3.45

Table 1 Area averaged surface variables and convective parameters for Simulations A and B at 1900Z and 2000Z.

4. CONVECTIVE EVOLUTION

The following discussion pertains to Simulation A. Convective initiation occurs on grid 4 over the Front Range mountains to the west of Denver and Fort Collins around 1830Z. These cells moved slowly northward with a maximum precipitation rate of approximately 2.5 cm/hr (~1 inch per hour). At 2000Z additional cells formed approximately 40 km to the southeast of Fort Collins and propagated northwestward at 5 m/s. These cells initiated on the eastern side of a surface wind speed boundary which formed as southeasterly surface winds increased over northeastern Colorado. By 2200Z these cells became quasi-stationary approximately 20 km to the southeast of Fort Collins. Maximum precipitation rates in this quasi-stationary system range from 14-19 cm/hr between 2200Z and 2300Z. At the same time, the storms to the southwest of Fort Collins which had developed over the Front Range mountains propagated north-eastward at around 10 m/s toward the quasi-stationary system. At 2300Z one of these northeastward-propagating cells merged with the quasi-stationary system and the resulting storm began propagating southeastward between 2300Z and 0000Z. By 0500Z, a maximum of 26 cm (10.23 inches) of precipitation had fallen 23 km to the southeast of Fort Collins. The simulation was terminated at this point since there was no indication of further precipitation occurring near the precipitation maximum.

In Simulation B, convection initiates at 1830Z over the Continental Divide southwest of Fort Collins. However, unlike Simulation A, no precipitating cells initiate east of the foothills before 2030Z. Rather, system formation occurs exclusively over the higher terrain in the western portion of Grid 4. Figure 1 shows the 12Z July 28 - 00Z July 29 accumulated precipitation on Grid 4 for Simulations A and B. Simulation B produces a much broader region of >10mm accumulation and several local maxima with magnitudes of 8-9 cm (3.1-3.5 in.). These maxima occur along a 140-km southwest-northeast oriented band that reflects the general motion of the northern component of the eastward propagating system. The maximum point-precipitation intensities are comparable between simulations with magnitudes between 100-180 mm/hr between 22Z and 00Z. The differences in accumulated precipitation magnitudes between simulations are largely due to variations in the propagation speeds of the simulated storms which appear to be correlated with the intensity and spatial extent of the storm-induced cold-pool.

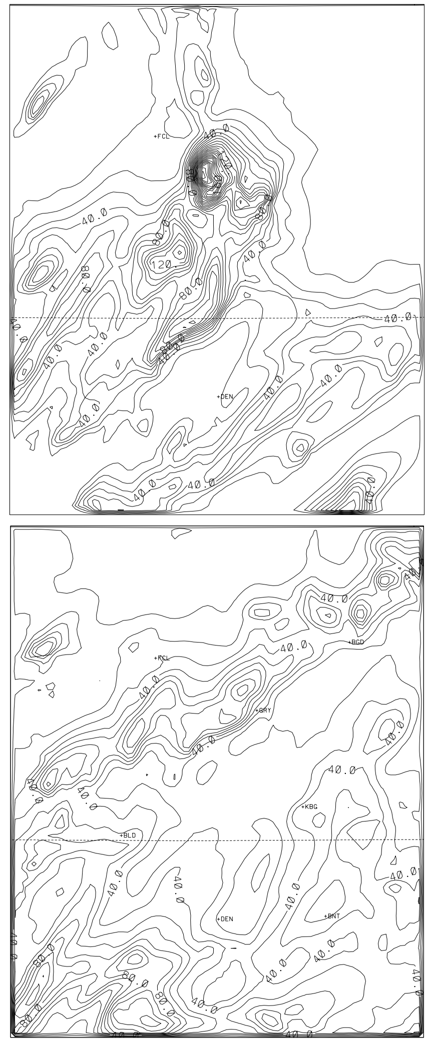

Figure 1. 12Z July 28-05Z July 29 accumulated precipitation for Sim. A (top) and Sim. B (bottom). Contour interval is 10 mm.

Figure 2 shows the low level potential temperature and precipitation rate at 2200Z when the flood producing storm in Sim. A is quasi-stationary and when the terrain initiated storms in Sim. B are in the vicinity of Fort Collins. This figure illustrates the differences in the strength and areal extent of the storm cold-pools. In Sim. B, the meso-β-scale cold-pool is nearly continuous between Fort Collins and Denver with two centers in the northern and southern half of the domain. Ultimately, this cold pool expands eastward, with new cells forming sporadically on the eastern flank. The resulting, ground-relative, system propagation vector is 5-6 m/s, eastward, between 21Z and 00Z. Individual cells move primarily north and northeastward at 10-12 m/s. In contrast, the simulated cold-pool, collocated with precipitation maximum in Sim. A, is meso-γ-scale, comparable in size to the actively precipitating region. Additionally, nowhere are the cold-pool potential temperature gradients comparable to those that occur on the eastern edge of the cold pool in Sim. B. Vertical profiles of the storm cold-pool perturbation potential temperatures corresponding to 2230Z are depicted in Figure 3. This plot shows that Sim. B produces a cold-pool with a larger negative buoyancy by a factor of 3-5, which extends approximately 1.7 km higher than that in Sim. A.

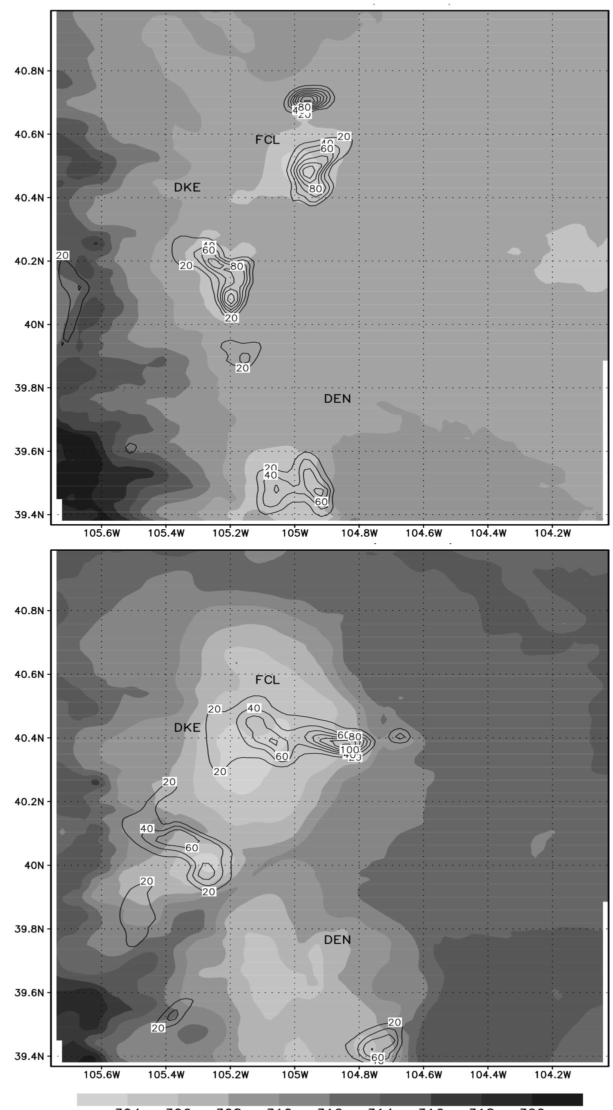

Figure 2. 22Z surface potential temperature and precipitation rate for Sim. A (top) and Sim. B (bottom). Precipitation rate contoured at 20 mm/hr intervals. Potential temperature shaded at 2K intervals.

In order to quantify the cold-pool strength, the conventional propagation speed for a 2-dimensional density current in an unsheared environment was computed: $c^2 = -2g \cdot \int \frac{\theta'}{\theta_0} dz$, where θ_0 is the upstream average potential temperature profile and θ' is the perturbation potential temperature profile at the cold-pool surface potential temperature minimum. A time series of this quantity for the simulated storms located ~20 km to the southeast of Fort Collins (not shown) indicated that *c* in Sim. A was typically within 2-3 m/s of the impinging easterly airflow and matched this windspeed during the quasi-stationary phase, while that of Sim. B exceeded the speed of the impinging airflow by 8-12 m/s. This agrees, qualitatively, with quasi-stationary character of the flood-producing storm in Sim. A compared to the persistent eastward movement of the cell-initiation locations and rapid extension of the cold-pool boundary in Sim. B..

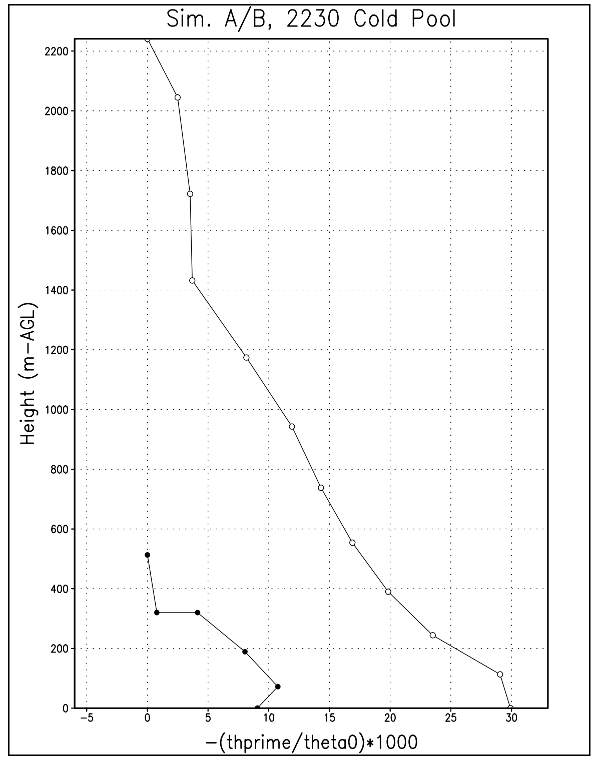

Figure 3. Plot of $-\frac{\theta'}{\theta_0} \cdot 10^3$ vs. height (m-AGL) at 2230Z for Simulations A (solid circles) and B (open circles).

Interestingly, a vertical profile of the absolute potential temperature of the cold-pools in Simulations A and B at 2230Z (Figure 4) shows that these profiles lie within 1K of each other at all levels extending to 3.9 km (MSL). An examination of the wind streamlines and theta-e cross-sections during the quasi-stationary phase of the flood-producing storm in Sim. A, showed that much of the cold-pool air originated above the boundary layer at 3-4 km (MSL). Hence the similarity of the cold-pool potential temperature profiles is likely due to the fact that the source air for the nearly saturated cold-pools originates within air which is relatively unaffected by the soil moisture initialization. The dissimilarity seen in the buoyancy profiles can be largely attributed to differences in the cold-pool boundary layer environment (i.e. the reference state). The warmer and deeper boundary layer in Sim. B results in a deeper and more negatively buoyant cold-pool despite the similarity in cold-pool absolute potential temperature profiles between simulations.

5. SUMMARY

The convective evolution of Sim. A and Sim. B were remarkably different. Simulation A exhibited explosive convective development between 20Z and 22Z over both the higher and lower elevations producing a quasi-stationary system at 22Z that released 26-cm of precipitation over a 5-6 hour period. Sim. B, however, developed convection initially only over the higher terrain, possibly a result of the reduced CAPE and the proximity of the LCL to the downslope westerly airflow at ~3200 m (MSL). No quasi-stationary systems developed in Sim. B. Examination of the storm-produced cold-pools showed that Sim. B produced a deeper and more negatively buoyant cold-pool. However, this was primarily due to the warmer and deeper boundary layer reference state — a direct result of the dryer soil moisture initialization in that simulation. This is also in agreement with the claims of Maddox et. al. (1978) and St. Amand et. al. (1972), in which the cool and moist surface conditions, and the resulting low LCL in the Big Thompson and Rapid City events, were deemed critical to the quasi-stationary characteristics of the storm due to weaker cold-pool formation. This study highlights a critical means of influence of soil moisture initialization on accumulated precipitation magnitudes through modulation of the cold-pool environment and the resulting cold-pool propagation speed.

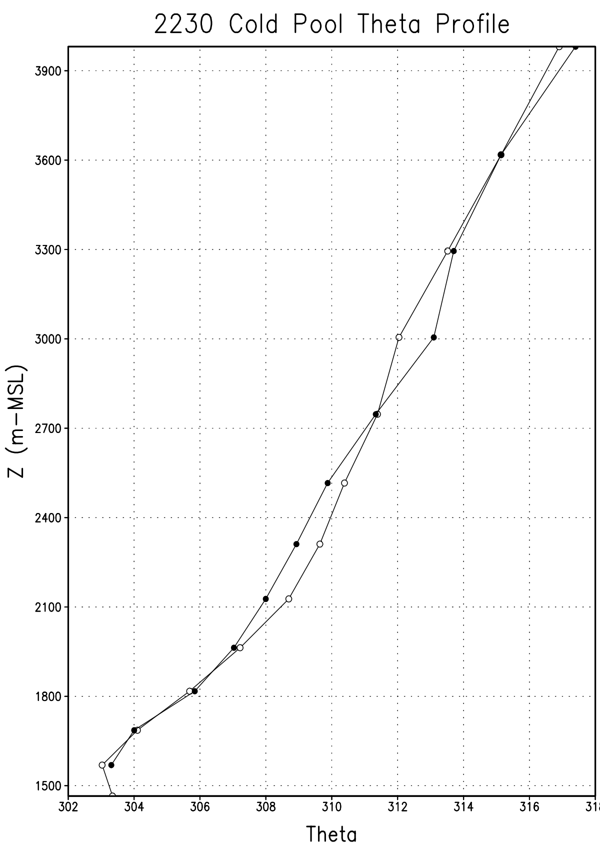

Figure 4. Potential temperature profile of cold-pools at 2230Z for simulations A and B.

Future modeling studies will investigate the dependence of simulated cold-pool structure and storm precipitation efficiency on user specified microphysical parameters such as cloud-droplet concentration and hail- and rain-diameters in the context of flash-flood producing environments.

This research is supported by the State of Colorado, Department of Natural Resources, Contract ENC#C154213.

6. REFERENCES

Doesken, N. J., and T.B. McKee, 1998: An analysis of rainfall for the July 28, 1997 flood in FCL, Colorado. Climatology Rep. 98-1, Department of Atmospheric Science, Colorado State University, 55 pp.

Maddox, R.A., L.R. Hoxit, C.F. Chappell, and F. Caracena, 1978: Comparison of meteorological aspects of the Big Thompson and Rapid City flash floods. *Mon. Wea. Rev.*, **106**, 375-389.

Petersen, W.A. and Coauthors, 1998: Mesoscale and radar observations of the Fort Collins flash flood of 28 July 1997. *Bull. Amer. Meteor. Soc.,* **80**, 191-216.

Pielke R.A. and Coauthors, 1992: A comprehensive meteorological modeling system -- RAMS. *Meteorol. Atmos. Phys.,* **49**, 69-91.

Saxton, K.E. and A.T. Lenz, 1967: Antecedent retention indexes predict soil moisture., *J. Hydraul. Div., Proc. Amer. Soc. Civ. Eng.*, **HY4**, 223-241.

St Amand, P., R.J. Davis and R.D. Elliot, 1972: Report on the Rapid City Flood of 9 June 1972. Report to South Dakota Weather Control Commission, Pierre, South Dakota, 37 pp.